Systematic Study on the Sensitivity Enhancement in Graphene Plasmonic Sensors Based on Layer-by-Layer Self-Assembled Graphene Oxide Multilayers and Their Reduced Analogues

Kyungwha Chung,[†] Adila Rani,[†] Ji-Eun Lee,[†] Ji Eun Kim,[‡] Yonghwi Kim,[§,⊥] Heejin Yang,[§] Sang Ouk Kim,[‡] Donghyun Kim,[§] and Dong Ha Kim*,[†]

[†]Department of Chemistry and Nano Science, Division of Molecular and Life Sciences, College of Natural Sciences, Ewha Womans University, Seoul, Republic of Korea

[‡]Center for Nanomaterials and Chemical Reactions, Institute for Basic Science (IBS), Department of Materials Science and Engineering, Korea Advanced Institute of Science and Technology (KAIST), Daejeon, Republic of Korea

[§]School of Electrical and Electronic Engineering, Yonsei University, Seoul, Republic of Korea

Ⓢ *Supporting Information*

ABSTRACT: The use of graphene in conventional plasmonic devices was suggested by several theoretic research studies. However, the existing theoretic studies are not consistent with one another and the experimental studies are still at the initial stage. To reveal the role of graphenes on the plasmonic sensors, we deposited graphene oxide (GO) and reduced graphene oxide (rGO) thin films on Au films and their refractive index (RI) sensitivity was compared for the first time in SPR-based sensors. The deposition of GO bilayers with number of deposition L from 1 to 5 was carried out by alternative dipping of Au substrate in positively- and negatively charged GO solutions. The fabrication of layer-by-layer self-assembly of the graphene films was monitored in terms of the SPR angle shift. GO-deposited Au film was treated with hydrazine to reduce the GO. For the rGO-Au sample, 1 bilayer sample showed a higher RI sensitivity than bare Au film, whereas increasing the rGO film from 2 to 5 layers reduced the RI sensitivity. In the case of GO-deposited Au film, the 3 bilayer sample showed the highest sensitivity. The biomolecular sensing was also performed for the graphene multilayer systems using BSA and anti-BSA antibody.

KEYWORDS: surface plasmon resonance (SPR) sensor, graphene plasmons, plasmonic coupling, sensitivity enhancement, refractive index sensing, layer-by-layer self-assembly
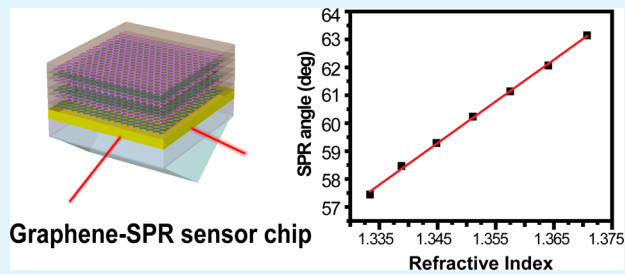
1. INTRODUCTION

Surface plasmon polaritons (SPPs) are the collectively oscillating charge densities at the interface between thin metal film and dielectrics in resonance with the incident light. Attractive properties of surface plasmon resonance (SPR) include (i) the amplified electromagnetic field at resonant frequency and (ii) energy confinement to the metal-dielectric interface in nanoscale dimension. In this regard, noble metal nanostructures which show SPR properties in visible ~ near-infrared range have been applied in various applications such as light-emitting enhancements,[1] visible light active photocatalysts,[2] photovoltaics,[3−5] optical biosensors,[6−8] etc. Among these applications, SPR-based sensors have emerged as a versatile tool for the label-free and real-time biomolecule sensing during the recent two decades.[7,9] However, it has been recognized that the sensitivity has yet to be improved to allow for single molecule detection. Incorporation of additional plasmonic nanostructures onto SPR sensor chip is one of the most promising strategies.[10] Metal nanoparticles with controlled sizes and lateral distances,[11,12] and plasmonic nanostructures such as

nanogratings[13] were employed in Kretschmann-configuration SPR sensors and the sensitivity enhancement was achieved because of the coupled field enhancement.

Another novel approach for the sensitivity enhancement of SPR-based sensors is the use of graphene. Graphene, single-atom-thick layer with sp²-bonded carbon atoms, having several distinctive properties such as high electronic and thermal conductivity, high quantum efficiency, and excellent mechanical strength, has attracted the attention of many scientific and industrial societies for the developments of optoelectronic devices.[14−20] Plasmons in graphene were also intensively investigated by some researchers and tight confinement, tunability and long propagation which make graphene as a promising material for SPP-based optical nanodevice applications were reported.[21−27] Furthermore, other advantageous features of graphene and its derivatives, such as large surface

area and strong interaction with biomolecules, have led to the use of graphene in biomedical applications.[28,29] Meanwhile, the excitation of graphene plasmons in the visible range is still remaining as the debating subjective.[30] Even though most of the graphene plasmonics have been demonstrated at terahertz frequency,[23,31] visible-light excitation is also theoretically expected.[32] However, it is required to enhance the light-matter interaction for the actual applications despite of relatively high light absorption of single layer graphene.[22] In this regard, the use of graphene in conventional plasmonic devices has been suggested.[22] For example, Wu et al. proposed graphene-Au film based SPR biosensor as one of the pioneering studies.[33] They performed numerical investigation and obtained the proportionate relationship between the number of graphene layer and the sensitivity due to strong and stable biomolecule adsorption and optical property of graphene. The sensitivity of graphene-on-Ag substrates in SPR imaging sensors have also been investigated.[34] In this study based on numerical analysis, the sensitivity decreased exponentially with increasing the number of graphene sheets and only less than 6 layers of graphene could enhance the sensitivity. Meanwhile, Verma et al. have tried to define the optimized structure for SPR-based sensors with a dielectric silicon layer.[35] Forty nanometer Au and 7 nm Si layers with graphene bilayer was assumed as the optimum structure for SPR sensors using 633 nm wavelength light. On the other hand, experimental observations were conducted using graphene synthesized by CVD method[36−41] or by electrochemical method,[42] graphene oxide (GO)[43−49] and reduced graphene oxide (rGO).[50−52] These studies mainly discussed that the sensitivity enhancement stemmed from large surface area and enhanced biomolecule attachment on graphene. Moreover, as the previous theoretical results are inconsistent one another in terms of the correlation between the number of graphene layers and the sensitivity of SPR-based sensors, fundamental and systematic experimental research on the contribution of graphene plasmonics to the sensitivity enhancement separating from other concurrent factors mentioned above is required and comparative study on the GO and rGO should also be carried out.

Meanwhile, layer-by-layer assembly is a facile and low-cost method to produce a thin film with well-defined thickness consisting of oppositely charged materials.[53] As chemically prepared GO sheets contain carboxylic acid, epoxide, and hydroxyl functional groups, formation of multilayer of GO with controllable thickness is not favored because of repulsive force. Thus, the introduction of positive charge on GO by either covalent bond formation of amine group or by coating with polyelectrolytes was developed in order to induce layer-by-layer (LbL) assembly.[54,55]

Herein, in this work, negatively charged GO, which is solution-processable and has tunability of the ratio of the sp^2 and sp^3 fractions by reduction, was prepared first and decorated with amine group to obtain positively charged GO. Multilayer graphene thin films were obtained by stepwise alternate deposition on Au films via layer-by-layer assembly. Bulk refractive index (RI) sensitivity and biomolecular recognition of GO-Au and rGO-Au substrates with different number of LbL deposition time were systematically compared in order to explore the sensitivity improvement induced by graphene-Au hybrid structures.

2. MATERIAL AND METHODS

2.1. Materials and Reagents. Graphite, sulfuric acid (H_2SO_4), sodium nitrate ($NaNO_3$), potassium permanganate ($KMnO_4$), barium chloride ($BaCl_2$), N-(3-(Dimethylamino)-propyl)-N′-ethylcarbodiimide hydrochloride (EDC), ethylamine, triethyl amine, bovine serum albumin (BSA, 98%), and antibovine albumin antibody (produced in rabbit, anti-BSA antibody, 4.8 mg mL^{-1}) were purchased from Sigma-Aldrich. All other chemical reagents were obtained from Daejung Chemicals (Korea).

2.2. Preparation of Graphene Oxides. Negatively charged graphene oxide (GO(−)) was prepared using the modified Hummer's method. Graphite flakes (2.5 g) were mixed with H_2SO_4 (57 mL) in a flask under vigorous stirring. $NaNO_3$ (1.5 g) was added in this mixture and stirred for 1 h, and then the dispersion was cooled to 0 °C in an ice bath. $KMnO_4$ (7.5 g) was added dropwise to the flask while maintaining the temperature below 20 °C followed by maintaining at 35 °C for 2 h. Cold deionized water was added slowly into the suspension. The mixture was stirred at 35 °C for 15 min and diluted by adding 350 mL of deionized water and 50 mL of 30% H_2O_2. Finally, the resulting yellow brown solution was centrifuged with a mixture of HCl and deionized water to remove the remaining metal ions until no sulfate ions were detected in a $BaCl_2$ solution test. The GO solution of light brown color was then washed repeatedly with deionized water until the pH of the filtrate became neutral. The resulting GO slurry was freeze-dried and stored in a desiccator. The required amount of GO was ultrasonicated in deionized water, centrifuged, and used as negatively charged graphene oxide (GO(−)). Positively charged GO (GO(+)) was prepared by using GO(−) suspension (50 mL), stirred for 4 h with EDC (500 mg), ethylamine (5 mL), and triethyl amine (1 mL), and then dialyzed for 24 h to eliminate unreacted reagents.

2.3. Layer-by-Layer (LbL) Deposition of GO on Au Film. Glass substrates with 2 nm thick Cr adhesion layer and 50 nm thick Au layer were used. The Au substrate was treated with O_2 plasma (100 W, 50 sccm, 10 min) and immersed in GO(+) solution (0.1 mg mL^{-1}) for 10 min, then rinsed with deionized water. After drying with nitrogen stream, the substrate was dipped in GO(−) solution (0.1 mg mL^{-1}) with the same immersion time and rinsing step. The immersion was conducted repeatedly until the desired thickness of assembled GO layers were obtained and the resulting multilayer was designated as $[GO(+)/GO(−)]_L$. L corresponds to the number of deposition of bilayer GOs ($L = 0−5$).

2.4. Reduction of GO on Au Film. LbL-assembled GO-Au film was treated by hydrazine vapor at 80 °C for 12 h.

2.5. Simulation. Calculation of GO thickness was carried out using Winspall software (RES-TEC, Germany) with complex refractive index value of $3 + 1.149106i$ for GO.[56] It was assumed that both the GO(+) and GO(−) have the same refractive index value.

2.6. Characterization of LbL Assembled GO-Au Film. The surface of the samples was investigated using field emission scanning electron microscopy (FE-SEM, JSM-6700F, JEOL) and atomic force microscopy (AFM, Dimension 3100, Veeco) in tapping mode.

2.7. SPR Measurements. SPR measurements (Resonant Technologies GmbH/RT2005 SPR spectrometer) were carried out using p-polarized laser light (He−Ne, 632.8 nm, 10 mW)
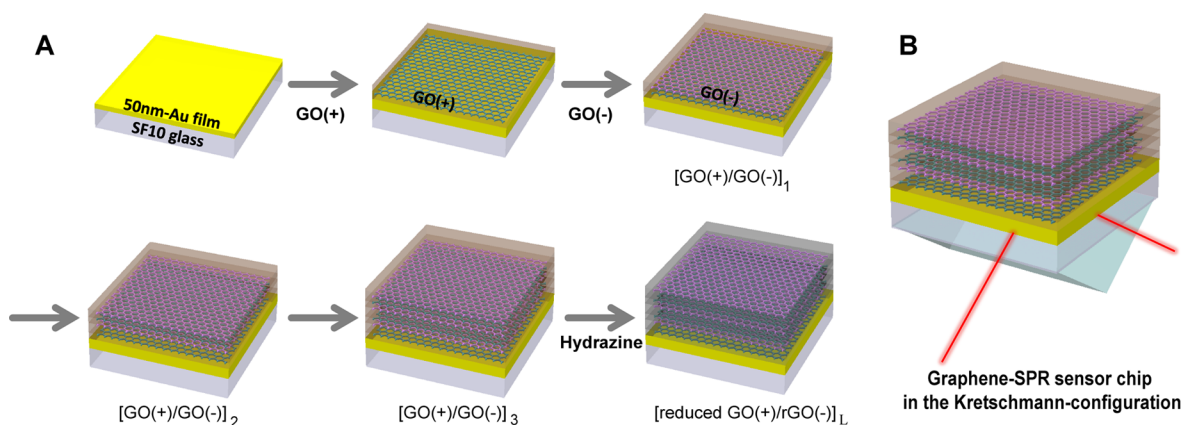
Figure 1. Schematic diagram of (A) GO deposition by LbL method and (B) Kretschmann configuration of GO-Au substrate.

illuminating the Au film through the LaSFN9 prism. All the SPR curves were collected in duplicate.

2.8. Sensing Experiments. Deionized water and glycerol solution with different concentrations (5−30 wt %) were used for the refractive index (RI) sensing (RI = 1.3334, 1.3388, 1.34481, 1.35106, 1.35749, 1.36404, 1.3707). After each solution was delivered to the sensing chamber, SPR angular scan was collected. SPR angles for each scan were determined using Winspall software.

Biomolecular sensing was carried out with BSA and anti-BSA antibody. BSA solution of 100 μg mL^{-1} was injected onto the graphene surface on Au film and adsorption was measured in situ. The binding event of anti-BSA antibody with concentrations of 6 μg mL^{-1} was also observed by in situ kinetic measurements at a fixed angle.

3. RESULTS AND DISCUSSION

3.1. Observation of LbL Assembly of GOs on Au Film. To deposit GO on Au film more efficiently and uniformly, pristine GO with hydroxyl, epoxy, and carboxylic acid functional groups and amine-functionalized GO were alternatively assembled on oxygen plasma-treated Au film by LbL assembly, as illustrated in Figure 1A.

The number of one bilayer deposition of GO(+) and GO(−) was varied from 0 (bare Au film) to 5, namely [GO(+)/GO(−)]$_L$-Au. To confirm the deposition process, [GO(+)/GO(−)]$_L$-Au sample was coupled with prism in Kretschmann configuration (Figure 1B) and SPR angular scan curve was measured ex situ (Figure 2A). The resonance angle shifted regularly as the LbL deposition was repeated and Figure 2B shows the linear correlation between L and SPR angles. An alternating deposition of one bilayer, i.e., GO(+) and GO(−), induced 0.12 ± 0.00242° of SPR angle shift. From the simulation study using Winspall software, we assume that around 1.2 nm thick GO layer was loaded on Au surface by one cycle of GO(+) and GO(−) LbL assembly.

3.2. Reduction of GO. The reduction of GO was carried out using hydrazine to investigate the effect of oxidation state of graphene on SPR sensitivity. [GO(+)/GO(−)]$_L$-Au samples were exposed to hydrazine vapor at 80 °C and the SPR angular curve was compared with the curve obtained from the identical sample before reduction (Figure 2C). This ex situ reduction method does not degrade Au-coated glass, whereas thermal reduction at 400 °C under Ar/H$_2$ atmosphere damaged it severely so that the glass substrate lost its transparency (see Figure S1 in the Supporting Information). As shown in Figure

2C, reduction of GO induced further SPR angle shift, indicative of the increase in the refractive index of graphene. This result is consistent with literatures which revealed that the complex RI ($N = n_1 + k_1i$) of GO was expressed with smaller value than that of rGO.[24,57] To confirm the reduction of GO, we measured Raman spectra. Characteristic Raman peaks of GO and rGO are confirmed as shown in Figure 3. The ratio between the intensities of the D and G peak (I_D/I_G) correlates with the disorder of graphene. I_D/I_G of GO is 1.05, whereas that of rGO is 1.55, indicating the successful reduction of graphene oxide on Au film using hydrazine vapor.

3.3. Surface Analysis of GO-Deposited SPR Chip and Angular Sensitivity. The surface of the samples was investigated by AFM images (Figures S2 and S3 and Table S1 in the Supporting Information) and SEM images (Figure 4A and Figure S4 in the Supporting Information). First of all, surface topology of GO(−) and GO(+) was studied (see Figure S2 in the Supporting Information). The thickness of the amine-functionalized GO(+) obtained from AFM height profile (see Figure S2D in the Supporting Information) was 1.45 nm, whereas the value of GO(−) was 1.11 nm (see Figure S1C in the Supporting Information), and more rough surface was observed on GO(+) than on GO(−), which is consistent with previously reported study.[54] Moreover, a decrease in surface roughness after reduction of GO was observed by AFM analysis (see Figure S3 in the Supporting Information). As summarized inTable S1 in the Supporting Information, after hydrazine treatment, average surface roughness of the sample was slightly decreased from 4.49 ± 0.67 nm to 4.04 ± 0.51 nm. More rough surface of GO(+)/GO(−) sample can be ascribed to the presence of oxygen-containing functional groups in GO(−) and amine groups in GO(+), leading to the higher interlayer spacing. On the other hand, for rGO layers, functional groups were partially eliminated by hydrazine and consequently slightly densified layer with smooth surface was obtained. This change in surface morphology after reduction was similarly observed in LbL-assembled GO after annealing at 1000 °C in H$_2$ atmosphere.[58] As revealed in the SPR angular curves in Figure 2A, it was observed by SEM images that repetitive LbL deposition led to an increase in the surface coverage (see Figure S3 in the Supporting Information). Particularly, relatively uniform deposition of GOs with large sizes was observed for the samples of [GO(+)/GO(−)]$_3$-Au (Figure 4A). An interesting feature of note in GO-Au composites is that their SPR angular scan curves almost did not show any broadening which is very common in nanostructures-incorporated Au film
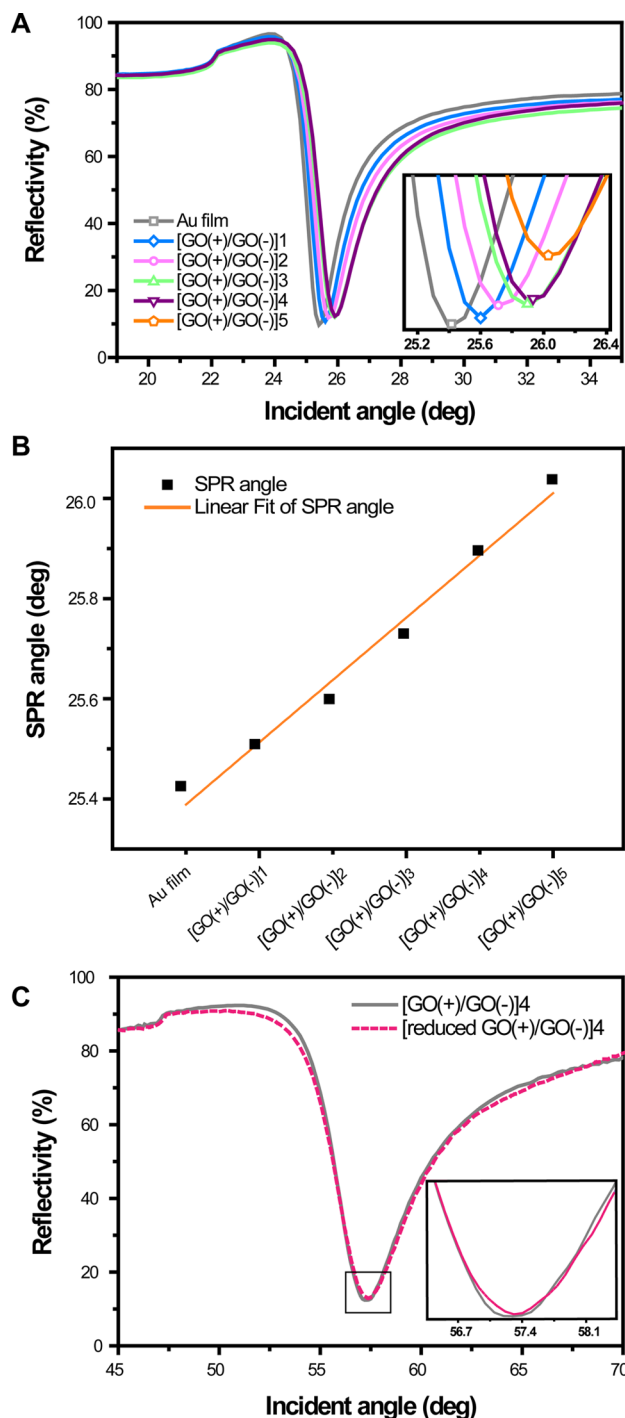
Figure 2. (A) SPR angular scan curves as a function of the GO(+)/GO(−) deposition number L, (B) relationship between the deposition number L and SPR angle positions and (C) SPR angular scan curves of $[GO(+)/GO(−)]_4$-Au before and after hydrazine treatment.

Figure 3. Raman spectra of $[GO(+)/GO(−)]_4$-Au (gray) and [reduced $GO(+)/GO(−)]_4$-Au (pink).

Figure 4. S(A) EM image of $[GO(+)/GO(−)]_3$-Au and (B) schematic representation for the evaluation of the figure of merit of Au film and $[GO(+)/GO(−)]_3$-Au.

$$FOM = \frac{\Delta R}{R_c} \frac{1}{FWHM} \qquad (1)$$

samples.[59] For highly sensitive SPR sensing devices, smaller full width at half-maximum (fwhm) value and deeper and narrower resonance spectrum are advantageous. Because of the atom-scale thickness of graphenes, the broadenings of curves and increases of reflectance at SPR angle position were barely observed, maintaining the resolution and figure of merit (FOM) as high as bare Au film (Figure 4B). FOM of SPR sensors is defined by Liu et al. as following eq 1[60]
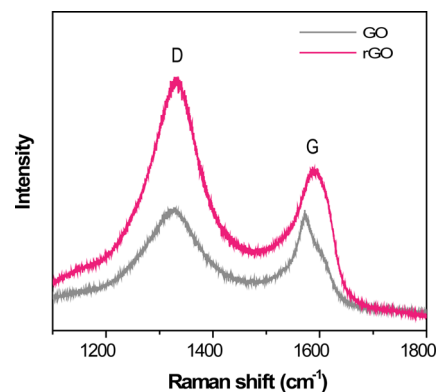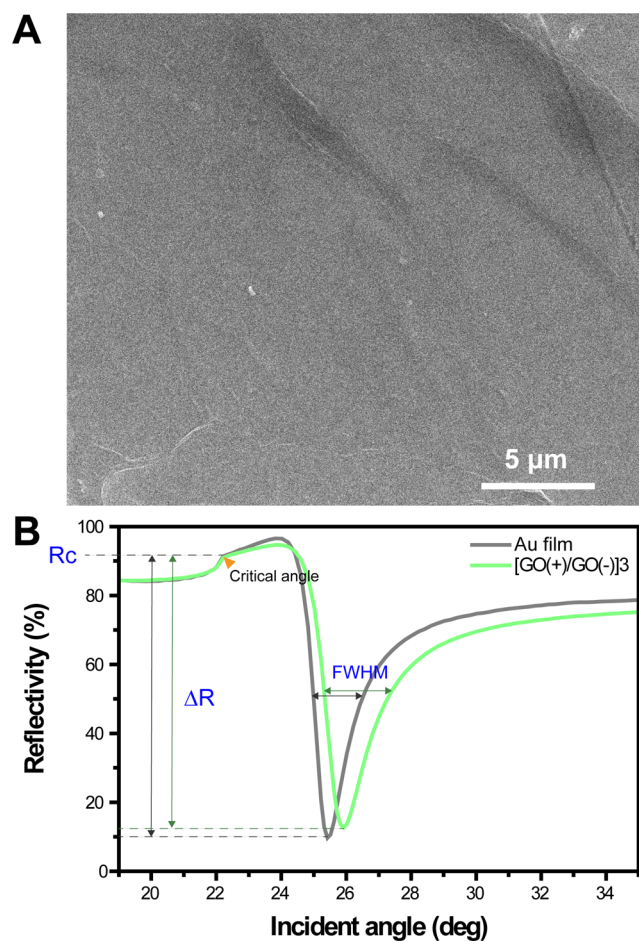
where ΔR is the difference in reflectivity between the critical angle and resonance angle, whereas R_c is the reflectivity at the critical angle. In the case of $[GO(+)/GO(−)]_3$-Au, in the aqueous medium, its FOM is measured to be 0.194 in our system, whereas the SPR curve of neat Au film in the aqueous medium showed 0.21 of FOM, which is comparable with GO-deposited samples.

3.4. Bulk Refractive Index Sensitivity. Previous works revealed that graphene can enhance the sensitivity by two factors: (i) increasing the attachment of biomolecules because of large surface area and (ii) increasing electromagnetic field. By demonstrating the bulk refractive index (RI) sensing by simply varying RI of the medium, which is irrelevant with any attachment of receptor and adsorption efficiency, electromagnetic contribution of GO and rGO can be deconvoluted. To investigate the bulk RI sensitivity, we introduced GO-Au or rGO-Au hybrid samples into the SPR spectrometer and the SPR angle shifts upon changing the concentration of aqueous glycerol solution were measured (Figure 5, Figure S5−S7 in the Supporting Information). The RI sensitivity is defined as the shift of SPR angle divided by the change in RI, which
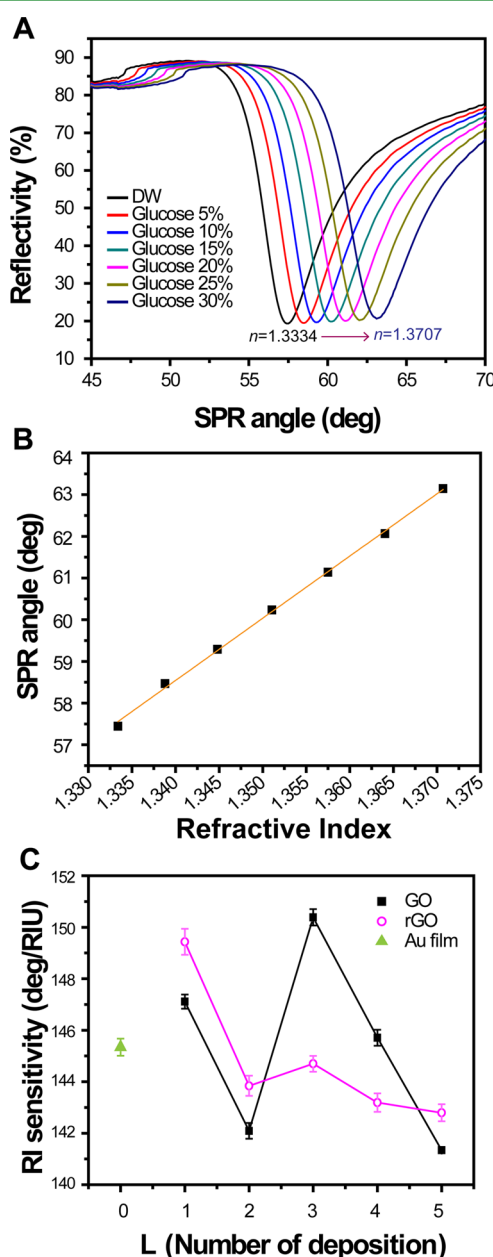

Figure 5. (A) Refractive index sensitivity of $[GO(+)/GO(-)]_3$-Au sample, (B) relationship between refractive index of medium and SPR angles, and (C) comparison of RI sensitivity obtained from different samples.

corresponds to the slope of the graph in Figure 5B. The RI sensitivity of all the samples with GO and rGO was compared with bare Au film as a function of the number of deposition in Figure 5C. $[GO(+)/GO(-)]_L$-Au for $L=$ 1, 3, and 4 and [reduced $GO(+)/GO(-)]_1$-Au showed higher sensitivity (147.11 ± 0.273, 150.38 ± 0.314, 145.71 ± 0.310 and 149.43 ± 0.504 deg RIU^{-1}, respectively) than neat Au film (145.34 ± 0.329 deg RIU^{-1}). Among these, $[GO(+)/GO(-)]_3$-Au samples showed the highest sensitivity, with RI sensitivity of 150.38 ± 0.314 deg RIU^{-1}, which is 3.45% higher than the bare Au substrate. For the GO-deposited samples, there was no clear correlation between L and the RI sensitivity. In the case of the [reduced $GO(+)/GO(-)]_L$-Au samples, a drastic downward trend in RI sensitivity is shown in Figure 5C when L was larger than 1, which is in agreement with a previous theoretic study[34] describing that the nonzero imaginary dielectric constant of graphene induced the damping of plasmons resulting in the decrease in sensitivity with increasing number of graphene layer. The sensitivity of our system is higher compared with the conventional SPR sensors with Kretschmann configuration which show typical RI sensitivity of 50−100 deg RIU^{-1},[61] and it is clearly demonstrated that the enhanced RI sensitivity of GO- and rGO-deposited samples is attributed to the optical properties of graphene. Xing et al. have also demonstrated that four layers of graphene on top of prism showed transverse magnetic (TM) mode sensitive behavior, which is similar to Au thin film in resonance condition with incident light, enabling RI sensing.[62] This reflects that graphene plasmons propagate at the interface of prism and media, and produce evanescent field, which is sensitive to the RI of environment. In this context, it can be concluded that the RI sensitivity enhancement was derived from coupling between propagating SPR, i.e., surface plasmon polaritons, and graphene plasmons.

3.5. BSA-anti-BSA Immunoreaction Sensing. Biomolecular sensing was further demonstrated using bovine serum albumin (BSA) and anti-BSA antibody (Figure 6). Control experiment was carried out with Au film, which was immersed in 1 mM mercaptopropionic acid (MPA) for 24 h in order to mimic GOs and to promote BSA attachment. BSA was first injected to the sample surface. The adsorption of BSA to the surface was observed by in situ kinetic measurements (Figure 6B, D, yellow curve). In both samples, the increased reflectivity after injecting BSA into the sensing chamber was observed in real time. The rinsing step was applied to remove improperly bound proteins, consequently resulting in a 3.3 and 2.5% increase in reflectivity from kinetic measurement and 0.10 and 0.09° of SPR angle shift in scan mode measurement, for the control and GO sample, respectively (Figure 6A, C, yellow curve). Then anti-BSA antibody was introduced to observe the binding kinetics between anti-BSA antibody and BSA. As shown in Figure 6D (blue curve), a sharp increase in reflectivity around 6% was obtained from GO sample due to the antigen−antibody reaction with high affinity (note that the molecular weight of antibody ($\sim$160 kDa) is higher than that of BSA (66 kDa)). It was found that the $[GO(+)/GO(-)]_3$-Au sample was capable of detecting 6 μg mL^{-1} of anti-BSA antibody with 0.2° of SPR angle shift, which corresponds to the mass sensitivity of 1430 pg mm^{-2}, indicating that this system shows the detection capability of the order of 7.15 pg mm^{-2} for an angular sensitivity of 1 mdeg. However, for the control sample, it showed only 0.5% increase in reflectivity in kinetic measurement (Figure 6B, blue curve) and 0.06° of SPR angle shift (Figure 6A, blue curve). SPR angle shift for BSA binding step in
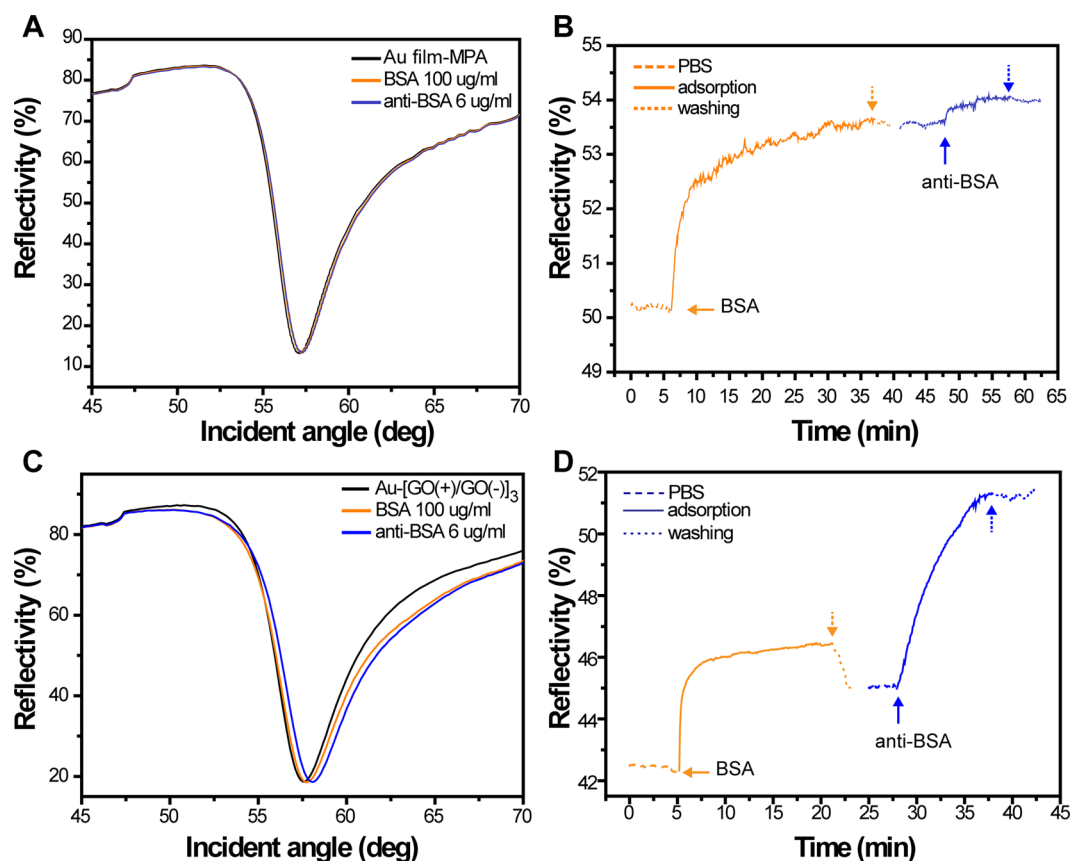
Figure 6. (A) BSA and anti-BSA sensing SPR angular scan curves and (B) in situ kinetic curves obtained using MPA-modified Au film and (C) SPR angular scan curves and (D) in situ kinetic curves obtained from $[GO(+)/GO(-)]_3$-Au.

both sensor chips was similar. However, $[GO(+)/GO(-)]_3$-Au chip exhibited 3.33 times higher sensitivity in anti-BSA antibody detection than control sample. It is conjectured that, in terms of anti-BSA antibody detection, this 3.33-fold enhancement in sensitivity was achieved through synergetic effect of graphene: (i) graphene plasmon coupling with Au film and (ii) the increased adsorption efficiency.

CONCLUSION

In summary, GO and rGO were introduced on gold film by LbL assembly and their effect on RI increase were systematically investigated. The recent development of SPR sensor chip with graphene was mainly focused on the improved attachment of receptor molecules and graphene layers were considered as dielectric material in theoretic studies. However, in this work, graphene plasmons couple with surface plasmon polaritons, resulting in amplification of evanescent field intensity and propagation length. This effect was supported by the observedenhanced RI sensitivity, while other factors such as the large surface area of graphene and improved adsorption efficiency of biomolecules were excluded. The coupling of graphene plasmons and surface plasmon polaritons induced higher sensitivity than conventional SPR sensor by simply depositing LbL assembled GO and the corresponding rGO on Au film. Moreover it was found that the FOM was almost maintained even after repetitive deposition of GO. Among the LbL assembled multilayer samples, the $[GO(+)/GO(-)]_3$-Ausample showed the best performance in RI sensing of 150.38 ± 0.314 deg RIU^{-1} and immunoreaction sensing was also conducted with a mass sensitivity of 7.15 pg mm^{-2} for anti-

BSA antibody corresponding to 1 mdeg angular sensitivity, which is enhanced by 3.33-fold compared with the control sample.

ASSOCIATED CONTENT

Ⓢ Supporting Information

Photograph of 50 nm thick Au-coated glass substrate and $GO(+)/GO(-)$-Au samples after thermal annealing; AFM images of $GO(-)$, $GO(+)$, Au film, $[GO(+)/GO(-)]_3$-Au sample, and [reduced $GO(+)/GO(-)]_3$-Au sample; SEM images of $[GO(+)/GO(-)]_L$-Au samples; refractive index sensing results of the $[GO(+)/GO(-)]_L$-Au samples, the [reduced $GO(+)/GO(-)]_L$-Au samples and bare Au film. This material is available free of charge via the Internet at http://pubs.acs.org.

AUTHOR INFORMATION

Corresponding Author

*E-mail: dhkim@ewha.ac.kr. Tel.: +82 2 3277 4517. Fax: +82 2 3277 3419.

Present Address

[⊥]Y.K. is currently at Department of Electrical Engineering, California Institute of Technology, Pasadena, California 91125, United States.

Notes

The authors declare no competing financial interest.

■ REFERENCES

(1) Kochuveedu, S. T.; Kim, D. H. Surface Plasmon Resonance Mediated Photoluminescence Properties of Nanostructured Multicomponent Fluorophore Systems. *Nanoscale* **2014**, *6*, 4966–4984.

(2) Kochuveedu, S. T.; Jang, Y. H.; Kim, D. H. A Study on the Mechanism for the Interaction of Light with Noble Metal-Metal Oxide Semiconductor Nanostructures for Various Photophysical Applications. *Chem. Soc. Rev.* **2013**, *42*, 8467–8493.

(3) Jang, Y. H.; Jang, Y. J.; Kochuveedu, S. T.; Byun, M.; Lin, Z.; Kim, D. H. Plasmonic Dye-Sensitized Solar Cells Incorporated with Au-TiO$_2$ Nanostructures with Tailored Configurations. *Nanoscale* **2014**, *6*, 1823–1832.

(4) Menezes, J. W.; Ferreira, J.; Santos, M. J. L.; Cescato, L.; Brolo, A. G. Large-Area Fabrication of Periodic Arrays of Nanoholes in Metal Films and Their Application in Biosensing and Plasmonic-Enhanced Photovoltaics. *Adv. Funct. Mater.* **2010**, *20*, 3918–3924.

(5) Atwater, H. A.; Polman, A. Plasmonics for Improved Photovoltaic Devices. *Nat. Mater.* **2010**, *9*, 205–213.

(6) Brolo, A. G. Plasmonics for Future Biosensors. *Nat. Photonics* **2012**, *6*, 709–713.

(7) Hoa, X. D.; Kirk, A. G.; Tabrizian, M. Towards Integrated and Sensitive Surface Plasmon Resonance Biosensors: A Review of Recent Progress. *Biosens. Bioelectron.* **2007**, *23*, 151–160.

(8) Willets, K. A.; Van Duyne, R. P. Localized Surface Plasmon Resonance Spectroscopy and Sensing. *Annu. Rev. Phys. Chem.* **2007**, *58*, 267–297.

(9) Homola, J.; Yee, S. S.; Gauglitz, G. Surface Plasmon Resonance Sensors: Review. *Sens. Actuators, B* **1999**, *54*, 3–15.

(10) Zeng, S.; Baillargeat, D.; Ho, H.-P.; Yong, K.-T. Nanomaterials Enhanced Surface Plasmon Resonance for Biological and Chemical Sensing Applications. *Chem. Soc. Rev.* **2014**, *43*, 3426–3452.

(11) Chung, K.; Lee, J.; Lee, J.-E.; Lee, J. Y.; Moon, S.; Lau, K. H. A.; Kim, D.; Kim, D. H. A Simple and Efficient Strategy for the Sensitivity Enhancement of DNA Hybridization Based on the Coupling between Propagating and Localized Surface Plasmons. *Sens. Actuators, B* **2013**, *176*, 1074–1080.

(12) Jang, Y. H.; Chung, K.; Quan, L. N.; Špačková, B.; Šípová, H.; Moon, S.; Cho, W. J.; Shin, H.-Y.; Jang, Y. J.; Lee, J.-E. Configuration-Controlled Au Nanocluster Arrays on Inverse Micelle Nano-Patterns: Versatile Platforms for SERS and SPR Sensors. *Nanoscale* **2013**, *5*, 12261–12271.

(13) Moon, S.; Kim, Y.; Oh, Y.; Lee, H.; Kim, H. C.; Lee, K.; Kim, D. Grating-Based Surface Plasmon Resonance Detection of Core-Shell Nanoparticle Mediated DNA Hybridization. *Biosens. Bioelectron.* **2012**, *32*, 141–147.

(14) Meyer, J. Carbon Sheets an Atom Thick Give Rise to Graphene Dreams. *Science* **2009**, *324*, 875–877.

(15) Geim, A. K.; Novoselov, K. S. The Rise of Graphene. *Nat. Mater.* **2007**, *6*, 183–191.

(16) Eda, G.; Fanchini, G.; Chhowalla, M. Large-Area Ultrathin Films of Reduced Graphene Oxide as a Transparent and Flexible Electronic Material. *Nat. Nanotechnol.* **2008**, *3*, 270–274.

(17) Balandin, A. A.; Ghosh, S.; Bao, W.; Calizo, I.; Teweldebrhan, D.; Miao, F.; Lau, C. N. Superior Thermal Conductivity of Single-Layer Graphene. *Nano Lett.* **2008**, *8*, 902–907.

(18) Li, X.; Zhang, G.; Bai, X.; Sun, X.; Wang, X.; Wang, E.; Dai, H. Highly Conducting Graphene Sheets and Langmuir–Blodgett Films. *Nat. Nanotechnol.* **2008**, *3*, 538–542.

(19) Park, C.-H.; Yang, L.; Son, Y.-W.; Cohen, M. L.; Louie, S. G. Anisotropic Behaviours of Massless Dirac Fermions in Graphene under Periodic Potentials. *Nat. Phys.* **2008**, *4*, 213–217.

(20) Bonaccorso, F.; Sun, Z.; Hasan, T.; Ferrari, A. Graphene Photonics and Optoelectronics. *Nat. Photonics* **2010**, *4*, 611–622.

(21) Gorbach, A. Nonlinear Graphene Plasmonics: Amplitude Equation for Surface Plasmons. *Phys. Rev. A* **2013**, *87*, 013830.

(22) Grigorenko, A.; Polini, M.; Novoselov, K. Graphene Plasmonics. *Nat. Photonics* **2012**, *6*, 749–758.

(23) Ju, L.; Geng, B.; Horng, J.; Girit, C.; Martin, M.; Hao, Z.; Bechtel, H. A.; Liang, X.; Zettl, A.; Shen, Y. R. Graphene Plasmonics for Tunable Terahertz Metamaterials. *Nat. Nanotechnol.* **2011**, *6*, 630–634.

(24) Jung, I.; Rhyee, J.-S.; Son, J. Y.; Ruoff, R. S.; Rhee, K.-Y. Colors of Graphene and Graphene-Oxide Multilayers on Various Substrates. *Nanotechnology* **2012**, *23*, 025708.

(25) Koppens, F. H.; Chang, D. E.; Garcia de Abajo, F. J. Graphene Plasmonics: A Platform for Strong Light–Matter Interactions. *Nano Lett.* **2011**, *11*, 3370–3377.

(26) Maier, S. A. Graphene Plasmonics: All Eyes on Flatland. *Nat. Phys.* **2012**, *8*, 581–582.

(27) Wang, B.; Zhang, X.; García-Vidal, F. J.; Yuan, X.; Teng, J. Strong Coupling of Surface Plasmon Polaritons in Monolayer Graphene Sheet Arrays. *Phys. Rev. Lett.* **2012**, *109*, 073901.

(28) Wang, Y.; Li, Z.; Wang, J.; Li, J.; Lin, Y. Graphene and Graphene Oxide: Biofunctionalization and Applications in Biotechnology. *Trends Biotechnol.* **2011**, *29*, 205–12.

(29) Bitounis, D.; Ali-Boucetta, H.; Hong, B. H.; Min, D. H.; Kostarelos, K. Prospects and Challenges of Graphene in Biomedical Applications. *Adv. Mater. (Weinheim, Ger.)* **2013**, *25*, 2258–2268.

(30) García de Abajo, F. J. Graphene Plasmonics: Challenges and Opportunities. *ACS Photonics* **2014**, *1*, 135–152.

(31) Fei, Z.; Andreev, G. O.; Bao, W.; Zhang, L. M.; S. McLeod, A.; Wang, C.; Stewart, M. K.; Zhao, Z.; Dominguez, G.; Thiemens, M.; Fogler, M. M.; Tauber, M. J.; Castro-Neto, A. H.; Lau, C. N.; Keilmann, F.; Basov, D. N. Infrared Nanoscopy of Dirac Plasmons at the Graphene–SiO$_2$ Interface. *Nano Lett.* **2011**, *11*, 4701–4705.

(32) Lange, P.; Kewes, G.; Severin, N.; Benson, O.; Rabe, J. P. Evidence for Graphene Plasmons in the Visible Spectral Range Probed by Molecules. *arXiv.org, e-Print Arch., Condens. Matter* **2014**, *1404*, 6518.

(33) Wu, L.; Chu, H.; Koh, W.; Li, E. Highly Sensitive Graphene Biosensors Based on Surface Plasmon Resonance. *Opt. Express* **2010**, *18*, 14395–14400.

(34) Choi, S. H.; Kim, Y. L.; Byun, K. M. Graphene-on-Silver Substrates for Sensitive Surface Plasmon Resonance Imaging Biosensors. *Opt. Express* **2011**, *19*, 458–466.

(35) Verma, R.; Gupta, B. D.; Jha, R. Sensitivity Enhancement of a Surface Plasmon Resonance Based Biomolecules Sensor Using Graphene and Silicon Layers. *Sens. Actuators, B* **2011**, *160*, 623–631.

(36) Kasry, A.; Ardakani, A. A.; Tulevski, G. S.; Menges, B.; Copel, M.; Vyklicky, L. Highly Efficient Fluorescence Quenching with Graphene. *J. Phys. Chem. C* **2012**, *116*, 2858–2862.

(37) Salihoglu, O.; Balci, S.; Kocabas, C. Plasmon-Polaritons on Graphene-Metal Surface and Their Use in Biosensors. *Appl. Phys. Lett.* **2012**, *100*, 213110.

(38) Kasry, A.; Afzali, A. A.; Oida, S.; Han, S.-J.; Menges, B.; Tulevski, G. S. Detection of Biomolecules via Benign Surface Modification of Graphene. *Chem. Mater.* **2011**, *23*, 4879–4881.

(39) Cai, H.; Cui, D.; Zhang, L. Surface Plasmon Resonance Characteristic Study of Graphene-on-Gold Structure. *12th IEEE Int. Conf. Nanotechnol.* **2012**, 1–3.

(40) Zagorodko, O.; Spadavecchia, J.; Serrano, A. Y.; Larroulet, I.; Pesquera, A.; Zurutuza, A.; Boukherroub, R.; Szunerits, S. Highly Sensitive Detection of DNA Hybridization on Commercialized Graphene-Coated Surface Plasmon Resonance Interfaces. *Anal. Chem.* **2014**, *86*, 11211–11216.

(41) Kravets, V. G.; Jalil, R.; Kim, Y. J.; Ansell, D.; Aznakayeva, D. E.; Thackray, B.; Britnell, L.; Belle, B. D.; Withers, F.; Radko, I. P.; Han, Z.; Bozhevolnyi, S. I.; Novoselov, K. S.; Geim, A. K.; Grigorenko, A. N. Graphene-Protected Copper and Silver Plasmonics. *Sci. Rep.* **2014**, *4*, 5517.

(42) Singh, V. V.; Gupta, G.; Batra, A.; Nigam, A. K.; Boopathi, M.; Gutch, P. K.; Tripathi, B. K.; Srivastava, A.; Samuel, M.; Agarwal, G. S. Greener Electrochemical Synthesis of High Quality Graphene Nanosheets Directly from Pencil and Its SPR Sensing Application. *Adv. Funct. Mater.* **2012**, *22*, 2352−2362.

(43) Zhang, H.; Sun, Y.; Gao, S.; Zhang, J.; Zhang, H.; Song, D. A Novel Graphene Oxide-Based Surface Plasmon Resonance Biosensor for Immunoassay. *Small* **2013**, *9*, 2537−2540.

(44) Zhang, J.; Sun, Y.; Xu, B.; Zhang, H.; Gao, Y.; Zhang, H.; Song, D. A Novel Surface Plasmon Resonance Biosensor Based on Graphene Oxide Decorated with Gold Nanorod−Antibody Conjugates for Determination of Transferrin. *Biosens. Bioelectron.* **2013**, *45*, 230−236.

(45) Huang, C.-F.; Yao, G.-H.; Liang, R.-P.; Qiu, J.-D. Graphene Oxide and Dextran Capped Gold Nanoparticles Based Surface Plasmon Resonance Sensor for Sensitive Detection of Concanavalin A. *Biosens. Bioelectron.* **2013**, *50*, 305−310.

(46) Zhang, J.; Sun, Y.; Wu, Q.; Zhang, H.; Bai, Y.; Song, D. A Protein a Modified Au−Graphene Oxide Composite as an Enhanced Sensing Platform for SPR-Based Immunoassay. *Analyst* **2013**, *138*, 7175−7181.

(47) Ryu, Y.; Moon, S.; Oh, Y.; Kim, Y.; Lee, T.; Kim, D. H.; Kim, D. Effect of Coupled Graphene Oxide on the Sensitivity of Surface Plasmon Resonance Detection. *Appl. Opt.* **2014**, *53*, 1419−1426.

(48) Chiu, N.-F.; Huang, T.-Y. Sensitivity and Kinetic Analysis of Graphene Oxide-Based Surface Plasmon Resonance Biosensors. *Sens. Actuators, B* **2014**, *197*, 35−42.

(49) Chiu, N.-F.; Huang, T.-Y.; Lai, H.-C.; Liu, K.-C. Graphene Oxide-Based SPR Biosensor Chip for Immunoassay Applications. *Nanoscale Res. Lett.* **2014**, *9*, 445.

(50) Wang, L.; Zhu, C.; Han, L.; Jin, L.; Zhou, M.; Dong, S. Label-Free, Regenerative and Sensitive Surface Plasmon Resonance and Electrochemical Aptasensors Based on Graphene. *Chem. Commun. (Cambridge, U. K.)* **2011**, *47*, 7794−6.

(51) Mao, Y.; Bao, Y.; Wang, W.; Li, Z.; Li, F.; Niu, L. Layer-by-Layer Assembled Multilayer of Graphene/Prussian Blue toward Simultaneous Electrochemical and SPR Detection of H_2O_2. *Talanta* **2011**, *85*, 2106−2112.

(52) Subramanian, P.; Lesniewski, A.; Kaminska, I.; Vlandas, A.; Vasilescu, A.; Niedziolka-Jonsson, J.; Pichonat, E.; Happy, H.; Boukherroub, R.; Szunerits, S. Lysozyme Detection on Aptamer Functionalized Graphene-Coated SPR Interfaces. *Biosens. Bioelectron.* **2013**, *50*, 239−243.

(53) Kovtyukhova, N. I.; Ollivier, P. J.; Martin, B. R.; Mallouk, T. E.; Chizhik, S. A.; Buzaneva, E. V.; Gorchinskiy, A. D. Layer-by-Layer Assembly of Ultrathin Composite Films from Micron-Sized Graphite Oxide Sheets and Polycations. *Chem. Mater.* **1999**, *11*, 771−778.

(54) Park, J. S.; Cho, S. M.; Kim, W. J.; Park, J.; Yoo, P. J. Fabrication of Graphene Thin Films Based on Layer-by-Layer Self-Assembly of Functionalized Graphene Nanosheets. *ACS Appl. Mater. Interfaces* **2011**, *3*, 360−8.

(55) Rani, A.; Oh, K. A.; Koo, H.; Lee, H. j.; Park, M. Multilayer Films of Cationic Graphene-Polyelectrolytes and Anionic Graphene-Polyelectrolytes Fabricated Using Layer-by-Layer Self-Assembly. *Appl. Surf. Sci.* **2011**, *257*, 4982−4989.

(56) Bruna, M.; Borini, S. Optical Constants of Graphene Layers in the Visible Range. *Appl. Phys. Lett.* **2009**, *94*, 031901.

(57) Jung, I.; Vaupel, M.; Pelton, M.; Piner, R.; Dikin, D. A.; Stankovich, S.; An, J.; Ruoff, R. S. Characterization of Thermally Reduced Graphene Oxide by Imaging Ellipsometry. *J. Phys. Chem. C* **2008**, *112*, 8499−8506.

(58) Lee, D. W.; Hong, T.-K.; Kang, D.; Lee, J.; Heo, M.; Kim, J. Y.; Kim, B.-S.; Shin, H. S. Highly Controllable Transparent and Conducting Thin Films Using Layer-by-Layer Assembly of Oppositely Charged Reduced Graphene Oxides. *J. Mater. Chem.* **2011**, *21*, 3438.

(59) Lyon, L. A.; Musick, M. D.; Smith, P. C.; Reiss, B. D.; Peña, D. J.; Natan, M. J. Surface Plasmon Resonance of Colloidal Au-Modified Gold Films. *Sens. Actuators, B* **1999**, *54*, 118−124.

(60) Liu, H.; Wang, B.; Leong, E. S.; Yang, P.; Zong, Y.; Si, G.; Teng, J.; Maier, S. A. Enhanced Surface Plasmon Resonance on a Smooth Silver Film with a Seed Growth Layer. *ACS Nano* **2010**, *4*, 3139−3146.

(61) Abdulhalim, I.; Zourob, M.; Lakhtakia, A. Surface Plasmon Resonance for Biosensing: A Mini-Review. *Electromagnetics* **2008**, *28*, 214−242.

(62) Xing, F.; Liu, Z. B.; Deng, Z. C.; Kong, X. T.; Yan, X. Q.; Chen, X. D.; Ye, Q.; Zhang, C. P.; Chen, Y. S.; Tian, J. G. Sensitive Real-Time Monitoring of Refractive Indexes Using a Novel Graphene-Based Optical Sensor. *Sci. Rep.* **2012**, *2*, 908.